Thin Solid Films 546 (2013) 436–438

Contents lists available at ScienceDirect

Thin Solid Films

journal homepage: www.elsevier.com/locate/tsf

Electronic structure of topological insulators with *MM′X* half-Heusler compounds using density functional theory

C. Li [a,b], Z. Wen [a,*]

[a] Key Laboratory of Automobile Materials (Jilin University), Ministry of Education, and School of Materials Science and Engineering, Jilin University, Changchun 130022, China
[b] School of Materials Science and Engineering, China Jiliang University, Hangzhou 330018, China

ARTICLE INFO

Available online 2 May 2013

Keywords:
Half-Heusler compounds
Topological insulator
Electronegativity

ABSTRACT

The band structures and partial density of states of *MM′X* half-Heusler compounds as topological insulators have been simulated by using local density approximate + *U*. Results show that both the covalent *M′–X* bonds and the ionic *M–M′* bands contribute the band structures, and the covalent bonds between *M′* and *X* atoms decide the number of $(E_{\Gamma 6} - E_{\Gamma 8})$ (Γ_6 and Γ_8 denote the twofold *s*-type orbitals and fourfold *p*-type orbitals and *M*, *M′*, and *X* show atoms located at different positions in the lattice); big size of $|\chi_{M'} - \chi_X|$ and small value of *V* are propitious to form topological insulators.

Crown Copyright © 2013 Published by Elsevier B.V. All rights reserved.

1. Introduction

Recently, a class of the so-called topological insulators (TIs) has been proposed theoretically and observed experimentally [1–4]. Differing from ordinary insulators, the TI with strong spin-orbit coupling and band inversion at Fermi level E_F is a state of quantum matters and has a full insulating gap in the bulk, but topologically protected gapless surface or edge states on the boundary. The TI is mostly used for quantum well and has possible application in spintronic devices [5,6].

Up to now, the search for TI behavior has been extended to ternary compounds: Heusler compounds [7–10], pyrochores [11], Kondo insulators [12], and thallium-based ternary chalcogenides [13], besides several binary compounds such as $Bi_{1-x}Sb_x$ alloy [14] and Bi_2Sb_3, Bi_2Te_3, and Sb_2Te_3 [15,16]. Since ternary compounds have one more element than binary ones, they have more selections to adjust $(E_{\Gamma 6} - E_{\Gamma 8})$ values by changing one of the components [7,8], where $(E_{\Gamma 6} - E_{\Gamma 8})$ is the energy difference between Γ_6 and Γ_8 bands at Γ point, and $(E_{\Gamma 6} - E_{\Gamma 8}) < 0$ denotes the appearance of the band-inversion. Similar to the well-known topological material HgTe, above ternary compounds show also the band inversion with topological order $Z_2 = -1$ [7,8].

To find more TIs, the nature of TIs has been studied widely, especially that of half-Heusler compounds (HHCs) [8,17]. For instances, an inert noble-gas atom Kr is added into HgTe and filled the void sites to form the ternary KrHgTe [8]. This does not change the topological nature of HgTe due to the fact that Kr atoms contribute to the band structure only through the addition of fully occupied bands lying well below the E_F. This artificial KrHgTe can then be transformed into a topological HHC by continuously changing the nuclear charge *Z*. Generally speaking, *MM′X* HHCs with the space group *F*43m can be viewed as a M^{n+} ion stuffing the zinc blende $M'X^{n-}$ sublattice (see Fig. 1 in Ref. [7]), where *M* and *M′* are metal elements, *X* denotes main-group element, and the structure can also be considered as being composed of three interpenetrating FCC lattices with positions described with the Wyckoff coordinates where atoms are arranged at the positions *M* (0.5, 0.5, 0.5), *M′* (0.25, 0.25, 0.25), and *X* (0, 0, 0). HHCs with 18 valence electrons in total ($n = 18$) have a closed atomic *K* shell ($d^{10}s^2p^6$). The number of $(E_{\Gamma 6} - E_{\Gamma 8})$ is in an inverse ratio with that of $(Z_{M'} + Z_X)V$ when the *M* and *X* lie III and V group atoms [8], where *V* is the unit-cell volume. However, these several HHCs fall short of the rule, such as when the *M* and *X* atoms lie in II and VI groups, this relation is absent, proving that the nature of forming TI is ambiguous due to complex relations among each component in HHCs. Understanding the nature of chemistry bonding will thus be propitious to find more TIs.

In this contribution, based on Lin et al.′s theory [8], we changed the nuclear charges $Z_{M'}$ and Z_X (*M* and *X* atoms lie in II and VI groups) to build several HHCs. First principles simulation was carried out to calculate the corresponding band structures, partial density of states (PDOS) and electronic configuration, and the results have been compared with present results.

2. Computational method

The band structure, PDOS, and electronic configuration of several HHCs were calculated based on the density functional theory

* Corresponding author. Fax: +86 431 85095876.
E-mail address: wenzi@jlu.edu.cn (Z. Wen).

0040-6090/$ – see front matter. Crown Copyright © 2013 Published by Elsevier B.V. All rights reserved.
http://dx.doi.org/10.1016/j.tsf.2013.04.066

with Perdew–Burke–Ernzerhof functional of generalized gradient approximation and with normconserving pseudopotentials [18], as implemented in CASTEP code [19]. Geometry optimizations of all materials are made on conventional unit cells using ultra-fine cutoff energies for the plane-wave expansion. The convergence tolerance of energy of 5.0×10^{-6} eV/atom, the maximum force of 0.01 eV/Å, and the maximum displacement of 5.0×10^{-4} Å were used. The *k*-point sampling set is $10 \times 10 \times 10$ division of the reciprocal unit cell based on the Monkhorst–Pack scheme [20]. Spin polarized and local density approximate (LDA) + *U* [21] have been used because LDA + *U* is now a well-established model to deal with electron correlations in transition or rare-earth metals, which guarantees the electronic structures of these materials being consistent with that of experimental results [22]. In LDA + *U* method, the strong correlation between localized *d*-electrons is explicitly taken into account through the screened effective electron–electron interaction parameter *U*.

3. Results and discussion

Fig. 1a gives the band structures of CaPtSe where gap at the Γ point is absent. The twofold degenerated Γ_6 states (dot line) lying down the fourfold degenerate Γ_8 states (dashed line) has an inverted band progression, being the necessary condition for TI state. CaPtSe changes the parity of the wave function (like HgTe) [1,11], and $(E_{\Gamma 6} - E_{\Gamma 8}) = -1.34$ eV. Based on Lin et al.'s theory, if we only change the nuclear charges Z_M' and Z_X, the materials should be the TIs with $Z_2 = -1$ once the lattice symmetry is broken by a uniaxial expansion along the [111] [8]. Fig. 1b shows PDOS of CaPtSe. The internal illustration in Fig. 1b shows the PDOS near E_F. The conduction band minimum consists of Se-4*p* and Pt-6*s* orbitals mostly, and the valence band maximum is composed of Se-4*p*, Pt-5*d*, and Pt-6*s* electrons, which is also shown in the electronic configuration of CaPtSe (Fig. 1c) where for orbitals at −3.9–0 eV (E_F is set at 0 eV), the orbitals around Se and Pt connect in the center of them as weak covalent bonds. Moreover, the electronic orbitals around Pt extrude along with Pt-Ca line, being obviously ionic Pt-Ca bonding, which affects the Pt-Se bonding. Also, the simulation analyses indicate that the charges transfer after the compound formation are $e_{Pt} = -1.38$, while $e_{Ca} = 1.35$ and $e_{Se} = 0.03$, where the subscripts denote the corresponding elements. Ca-3*s* electrons are transferred to Pt or Se. Moreover, some Pt-5*d*, Pt-6*s*, Se-4*p*, and Ca-3*s* electrons hybridize together and form a new bonding orbital between −6.3 and −4.8 eV in Fig. 1b. and when the orbitals are at −6.3 to −4.8 eV in Fig. 1c, almost all electrons are fixed between Pt and Se atoms, which definitely proves the existence of strong covalent spd^2 hybridization of Pt-5*d*, Pt-6*s*, Se-4*p*, and Ca-3*s* electrons where each Pt atom has fourfold covalent bonds with four Se atoms, and the total number of valence electrons is six here. Moreover, for orbitals at −4.5 to −3.9 eV in Fig. 1c, about four *d* electrons surround Pt atom, which shows obvious lone pair electron characteristic. All considered materials have similar results. As only one band inversion occurs at the Γ point of the Brillouin zone, these three-dimensional materials belong to the strong-TI class within a Fu-Kane-type classification scheme by the adiabatic argument [23].

To compare influences of different *U* values on the electronic structure, we calculate all considered materials with different *U* values. Taking CaPtSe as an example, we change the *U* values of Pt atom. The results of corresponding band structures calculated for $E_{\Gamma 6} - E_{\Gamma 8}$ are shown in Fig. 2. It is found that the values of $E_{\Gamma 6} - E_{\Gamma 8}$ decrease as the *U* values of Pt atom increase from 1 to 6 eV. When $U = 6$–8 eV, the values of $E_{\Gamma 6} - E_{\Gamma 8}$ change little. Thus, $U = 6$ eV for Pt atom could be adequate to deal with electron correlations. Note that when $U = 0$, CaPtSe becomes a conductor, which implies that LDA + *U* technique is necessary for the simulation in our case. All considered materials have the same results of the above. Thus, $U = 6$ eV is taken for Pt atom.

Fig. 3a shows the relationships between $(E_{\Gamma 6} - E_{\Gamma 8})$ and $(Z_M' + Z_X)V$ values of several TIs. As shown in the figure, when the *M* and *X* atoms lie in II and VI groups, the number of $(E_{\Gamma 6} - E_{\Gamma 8})$ has a direct ratio with the number of $(Z_M' + Z_X)V$, which are different from

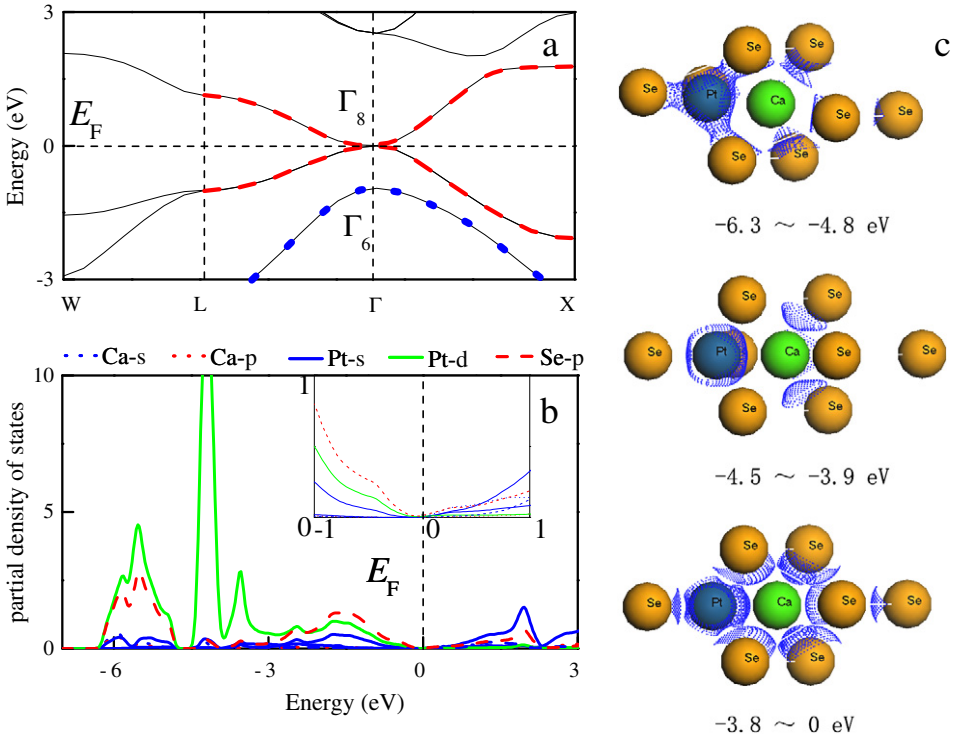

Fig. 1. (a) Band structures and (b) PDOS of CaPtSe, where the dot line marks the bands with Γ_6 symmetry and the dash line is Γ_8 symmetry. (c) Electronic configuration of CaPtSe at different energy levels.

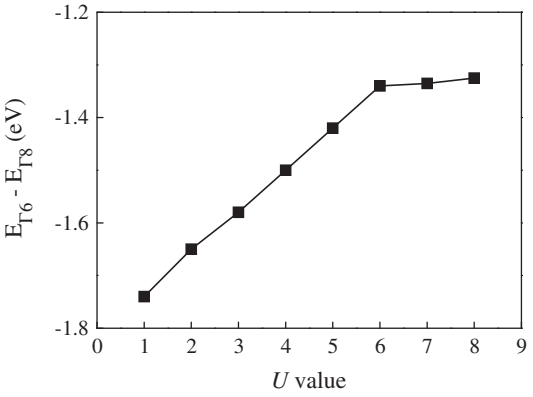

Fig. 2. The energy difference between Γ_6 and Γ_8 bands ($E_{\Gamma6} - E_{\Gamma8}$) of CaPtSe as a function of different U values of Pt atom.

other's results [6]: when the M and X atoms lie in III and V groups, the number of ($E_{\Gamma6} - E_{\Gamma8}$) is in inverse ratio with that of $(Z_{M'} + Z_X)V$. As already pointed by Ogüchi [24], the band structure near the E_F at the Γ point is determined mainly by $M'X$ with the zinc blende structure, the covalent bonds between M' and X atoms thus may be related to the number of ($E_{\Gamma6} - E_{\Gamma8}$). However, it is obvious that the values of the absolute difference of Pauling electronegativities between M' and X atoms $|\chi_{M'} - \chi_X|$ and V are related to the covalent bonds, where χ values of corresponding atoms are given in Table 1. Therefore, let $|\chi_{M'} - \chi_X| / V$ express the covalent bonds between M' and X atoms, and the relationships between ($E_{\Gamma6} - E_{\Gamma8}$) and $|\chi_{M'} - \chi_X| / V$ are shown in Fig. 3b. We can find that this has the same trend for M'

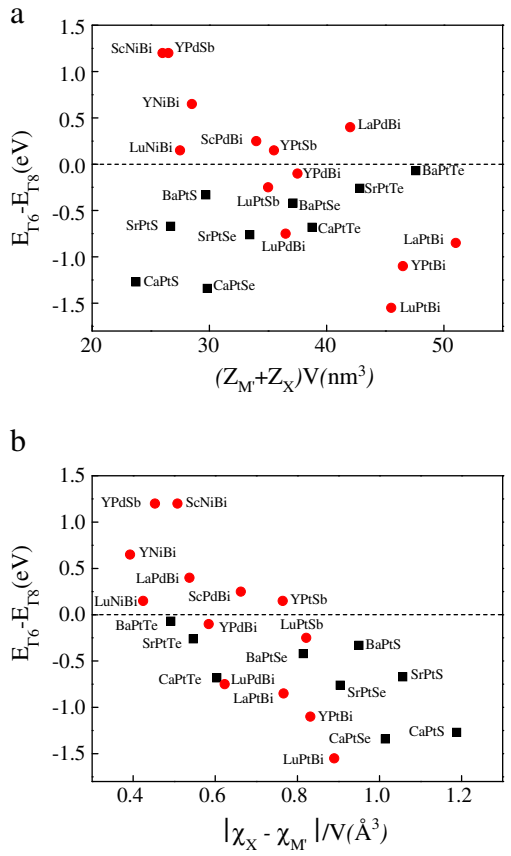

Fig. 3. Relationships (a) between ($E_{\Gamma6} - E_{\Gamma8}$) and $(Z_{M'} + Z_X)V$ and (b) between ($E_{\Gamma6} - E_{\Gamma8}$) and $|\chi_{M'} - \chi_X| / V$ where the symbol ■ denotes our results and ● are cited from references [8].

Table 1
The corresponding Pauling electronegativities χ of all atoms [25].

Atom	Ni	Pd	Pt	S	Se	Te	Sb	Bi
χ	1.91	2.20	2.28	2.58	2.55	2.10	2.05	2.02

and X atoms lying in II and VI groups or lying in III and V groups, it shows when these HHCs have the same M elements, larger value of $|\chi_{M'} - \chi_X|$ and smaller V value denote larger number of ($E_{\Gamma6} - E_{\Gamma8}$). So the covalent bonds between M' and X atoms decide the number of ($E_{\Gamma6} - E_{\Gamma8}$), larger value of $|\chi_{M'} - \chi_X|$, and smaller V value benefit for forming TIs, the covalent bonding are not benefit for forming TIs in some certain range.

In summary, band structures, PDOS, and electronic configuration of CaPtSe HHCs have been simulated using LDA + U. The results show that both the covalent M'–X bonds and the ionic M–M' bands contribute the band structures. When more HHCs are compared, it is found that the covalent bonds between M' and X atoms decide the number of ($E_{\Gamma6} - E_{\Gamma8}$), while larger $|\chi_{M'} - \chi_X|$ value and smaller V value benefit for forming TIs.

Acknowledgments

The authors acknowledge the financial support from the NNSFC (grant no. 50571040), the National Key Basic Research and Development Program (grant no. 2010CB631001), the Program for Changjiang Scholars and Innovative Research Team in University, and the High Performance Computing Center (HPCC) of Jilin University for supercomputer time.

References

[1] B.A. Bernevig, T.L. Hughes, S.C. Zhang, Science 314 (2006) 1757.
[2] M. Konig, S. Wiedmann, C. Brune, A. Roth, H. Buhmann, L. Molenkamp, X.-L. Qi, S.-C. Zhang, Science 318 (2007) 766.
[3] Y.P. Jiang, Y.L. Wang, M. Chen, C.L. Song, K. He, L.L. Wang, X. Chen, X.C. Ma, Q.K. Xue, Phys. Rev. Lett. 108 (2012) 016401.
[4] R. Roy, Phys. Rev. B 79 (2009) 195322.
[5] X.-L. Qi, S.-C. Zhang, Phys. Today 63 (2010) 33.
[6] D. Kong, Y. Cui, Nat. Chem. 3 (2011) 845.
[7] S. Chadov, X.L. Qi, J. Kübler, G.H. Fecher, C. Felser, S.C. Zhang, Nat. Mater. 9 (2010) 541.
[8] H. Lin, L.A. Wray, Y.Q. Xia, S.Y. Xu, S. Jia, R.J. Cava, A. Bansil, M.Z. Hasan, Nat. Mater. 9 (2010) 546.
[9] C. Li, J.S. Lian, Q. Jiang, Phys. Rev. B 83 (2011) 235125.
[10] M. Franz, Nat. Mater. 9 (2010) 536.
[11] D.A. Pesin, L. Balents, Nat. Phys. 6 (2010) 376.
[12] M. Dzero, K. Sun, V. Galitski, P. Coleman, Phys. Rev. Lett. 104 (2010) 106408.
[13] S.V. Eremeev, G. Bihlmayer, M. Vergniory, Yu.M. Koroteev, T.V. Menshchikova, J. Henk, A. Ernst, E.V. Chulkov, Phys. Rev. B 83 (2011) 205129.
[14] D. Hsieh, D. Qian, L. Wray, Y. Xia, Y.S. Hor, R.J. Cava, M.Z. Hasan, Nature 452 (2008) 970.
[15] Y.L. Chen, J.G. Analytis, J.-H. Chu, Z.K. Liu, S.-K. Mo, X.L. Qi, H.J. Zhang, D.H. Lu, X. Dai, Z. Fang, S.C. Zhang, I.R. Fisher, Z. Hussain, Z.-X. Shen, Science 325 (2009) 178.
[16] Y. Xia, D. Qian, D. Hsieh, L. Wray, A. Pal, H. Lin, A. Bansil, D. Grauer, Y.S. Hor, R.J. Cava, M.Z. Hasan, Nat. Phys. 5 (2009) 398.
[17] D. Xiao, Y.G. Yao, W.X. Feng, J. Wen, W.G. Zhu, X.-Q. Chen, G.M. Stocks, Z.Y. Zhang, Phys. Rev. Lett. 105 (2010) 096404.
[18] D.R. Hamann, M. Schluter, C. Chiang, Phys. Rev. Lett. 43 (1979) 1494.
[19] J.P. Perdew, K. Burke, M. Ernzerhof, Phys. Rev. Lett. 77 (1996) 3865.
[20] H.J. Monkhorst, J.D. Pack, Phys. Rev. B 13 (1976) 5188.
[21] I.V. Solovyev, P.H. Dederichs, V.I. Anisimov, Phys. Rev. B 50 (1994) 16861.
[22] M. Cococcioni, S. Gironcoli, Phys. Rev. B 71 (2005) 035105.
[23] L. Fu, C.L. Kane, Phys. Rev. B 76 (2007) 045302.
[24] T. Ogüchi, Phys. Rev. B 63 (2001) 125115.
[25] A.M. James, M.P. Lord, Macmillan's Chemical and Physical Data, Macmillan, London, UK, 1992.